


 Cite this: *RSC Adv.*, 2025, **15**, 32328

Extraction and determination of esteric compounds in wound disinfectants

 Mir Ali Farajzadeh, *^{ab} Zahra Hallaji,^a Sakha Pezhhanfar^a
 and Mohammad Reza Afshar Mogaddam ^{cde}

This study focuses on developing an analytical method to efficiently extract and concentrate several adipate and phthalate plasticizers that can migrate from plastic packaging into various wound disinfectants. The study employed an approach that combined dispersive micro solid phase extraction with dispersive liquid–liquid microextraction using ZIF-4 as an adsorbent. The adsorbent was thoroughly characterized to understand its properties. The microextraction step concentrated the target compounds for analysis using gas chromatography. After plasticizer adsorption onto ZIF-4, the analytes were desorbed using acetonitrile. The method demonstrated good performance by high extraction recoveries (61–95%) and enrichment factors (305–475), low detection (0.16–0.28 $\mu\text{g L}^{-1}$) and quantification (0.54–0.93 $\mu\text{g L}^{-1}$) limits, and good precision (relative standard deviation less than 7% for intra- and inter-day precisions).

 Received 6th May 2025
 Accepted 27th August 2025

DOI: 10.1039/d5ra03198b

rsc.li/rsc-advances

1 Introduction

Plastic has become an integral component of contemporary society, pervading numerous aspects of daily life.^{1,2} Plastic's lightweight design, flexibility, ease of handling, and affordability have made it ubiquitous in our lives. From food packaging to medical equipment, it offers undeniable benefits.³ Most plastic polymers contain different additives like antioxidants, plasticizers, and colorants. These additives play critical roles in both processing efficiency and the final products' performance characteristics such as durability, flexibility, and aesthetics.⁴ Several types of phthalate esters are commonly used as plasticizers, including di(2-ethylhexyl) phthalate (DEHP), di-*n*-butyl phthalate (DIBP), and di-*n*-butyl phthalate (DNBP), along with di(2-ethylhexyl) adipate (DEHA).⁵ For instance, DEHA is frequently found in the polyvinyl chloride films used in food wrapping and drug containers.⁶ Even polyethylene terephthalate bottles, commonly used for beverages, can contain varying amounts of phthalate esters. The critical factor resides in the weak intermolecular interactions exhibited between plasticizers and the polymer chains.⁷ Instead, only weak

physical interactions bond them to each other. Studies have implicated phthalates in a spectrum of health concerns, including reproductive dysfunction, endocrine disruption, male infertility, dermatological conditions, obesity, and metabolic disorders. Nephrotoxicity and hepatotoxicity have been observed even with low-level and chronic phthalate exposure.^{8,9} These potential health risks have led to increased attention from international regulators.¹⁰ Studies have shown how important it is to accurately detect and measure phthalates to ensure product safety and protect human health. Traditionally, gas chromatography (GC)^{11,12} and high performance liquid chromatography (HPLC)^{13,14} have been the main methods used to analyze plasticizers in different materials. However, GC can not be used in aqueous samples, and HPLC can be negatively affected by the sample itself and result in trouble. Therefore, initially, it is inevitable to perform sample preparation steps. Sample preparation methods like liquid–liquid extraction^{15,16} and solid phase extraction (SPE)^{17,18} were used to concentrate and purify the analytes before chromatographic analyses. In recent years, there has been a shift towards more efficient and compact sample preparation techniques. Methods like dispersive liquid–liquid microextraction (DLLME)^{19–21} and its variations have gained popularity due to their ability to preconcentrate analytes from complex matrices, often with reduced solvent consumption and improved sensitivity compared to traditional methods. To address the limitations of conventional SPE, such as cartridge clogging, dispersive micro solid phase extraction (D μ SPE)^{22,23} was developed. These advancements collectively contribute to improved analyte extraction recovery (ER) and enrichment factor (EF), ultimately enhancing the overall analytical performance.

^aDepartment of Analytical Chemistry, Faculty of Chemistry, University of Tabriz, Tabriz, Iran. E-mail: mafarajzadeh@yahoo.com; mafarajzadeh@tabrizu.ac.ir; Fax: +98 41 33340191; Tel: +98 41 33393084

^bEngineering, Faculty, Near East University, 99138 Nicosia, North Cyprus, Mersin 10, Turkey

^cFood and Drug Safety Research Center, Pharmaceutical Sciences Institute, Tabriz University of Medical Sciences, Tabriz, Iran

^dResearch Center of New Material and Green Chemistry, Khazar University, 41 Mehseti Street, Baku AZ1096, Azerbaijan

^ePharmaceutical Analysis Research Center, Pharmaceutical Sciences Institute, Tabriz University of Medical Sciences, Tabriz, Iran



Metal–organic frameworks (MOFs), renowned for their exceptional properties such as extensive surface area and customizable structures, represent a revolutionary class of materials.^{24,25} Their versatility has driven their application across diverse fields including environmental remediation, energy storage, and drug delivery. Analytical chemistry employs MOFs in chromatography and sample preparation. Some MOFs, such as MOF-5,²³ UMCM-1,²⁵ and NiGA,²⁶ have shown promise in the extraction and preconcentration of plasticizers. Zeolitic imidazolate framework (ZIF) is a well-known type of MOF that is highly stable under heat and it is chemically resistant. It is also an excellent material for creating hollow nanostructures.

In this study, ZIF-4 was successfully synthesized and characterized as an MOF. Subsequently, ZIF-4 was effectively employed in a combined D μ SPE-DLLME process to extract and preconcentrate some plasticizers including DEHA, DEHP, DIBP, and DNBP from various wound disinfectant samples. The main innovation of this method is the first time use of ZIF-4 as an adsorbent in a sensitive analytical technique for extraction of various plasticizers. Additionally, its rapid release of the captured plasticizers enhances the overall efficiency of the analytical process.

2 Experimental

2.1 Chemicals and solutions

Imidazole, *N,N*-dimethylformamid (DMF), and zinc nitrate hexahydrate, all obtained from Merck (Darmstadt, Germany), were used in the ZIF-4 synthesis. The target analytes consisting of DNBP, DIBP, DEHP, and DEHA were prepared from Sigma-Aldrich (St. Louis, MO, USA). Hydrochloric acid (37%, w/w) and sodium hydroxide obtained from Merck were employed for pH adjustments of solutions. Deionized water was provided from Ghazi Co, (Tabriz, Iran). Sodium sulfate, sodium chloride, acetonitrile (ACN), methanol, 1-propanol, and 2-propanol were obtained from Merck. Analytical grade extraction solvents, including chloroform, 1,2-dibromoethane (1,2-DBE), and 1,1,1-trichloroethane (1,1,1-TCE), procured by Janssen (Beerse, Belgium) were utilized in this study. Deionized water was used to dilute a methanolic stock solution at a concentration of 500 mg L⁻¹ of each analyte.

2.2 Samples

Three different wound disinfectant solutions were obtained from a pharmacy in Tabriz, Iran. All samples were stored at room temperature before being used in the proposed method. To prepare the samples for analysis, deionized water was employed for diluting the samples at a ratio of 1 : 4 (deionized water : disinfectant).

2.3 Apparatus

To detect and measure esteric compounds, a Shimadzu GC-FID (model 2014) device with a split/splitless inlet system (Kyoto, Japan) was used. The chromatographic separation was performed on a Zebtron capillary column (30 m \times 0.25 mm i.d., 0.25 μ m film thickness) composed of 95% dimethyl and 5% diphenyl

polysiloxane (Phenomenex, Torrance, CA, USA). The GC system was optimized at the temperature of 300 °C for both the injection port and FID. Sampling time of 1 min, and a split ratio of 1 : 10 were employed. A temperature programming was applied in the column oven, starting at 60 °C for 1 min and increasing to 300 °C at a rate of 18 °C min⁻¹, followed by a holding time of 3 min at the end of the separation process. Helium (99.999%, Gulf Cryo, Dubai, United Arab Emirates) was used as the carrier (30 cm min⁻¹) and makeup gas (30 mL min⁻¹) gases, while air and hydrogen were employed for the FID. A Zebtron capillary column was used for separation. GC-(mass spectrometry) MS analysis was conducted on a Shimadzu GC-MS-QP2010 plus instrument. The GC-MS separation was performed using a Phenomenex, Zb-35 HT capillary column (20 m \times 0.18 mm i.d., a film thickness of 0.18 μ m). Helium was used as the carrier gas with a flow rate of 0.66 mL min⁻¹. The oven temperature programming began at 60 °C, held for 2.0 min, ramped to 300 °C at a rate of 20 °C min⁻¹, and finally held for 6.0 min. The injection port temperature for the GC-MS system were identical to that used in the GC-FID system. A Hettich centrifuge and an L46 vortex were used in sample preparation. A Metrohm pH meter model 654 was employed for pH measurement.

2.4 ZIF-4 synthesis

A previously described method was used to synthesize ZIF-4.²⁷ Zinc nitrate hexahydrate (1.37 g) and imidazole (0.9 g) underwent dissolution in 40 mL of DMF. The solution was stirred for 10 min. After its transferring into a 100 mL autoclave, it was sealed tightly and underwent a solvothermal reaction at 130 °C for 48 h in an oven. The cooled autoclave was stored overnight, followed by washing the synthesized product with DMF (3 \times 50 mL) and drying it on filter paper overnight.

2.5 Extraction procedure

Each analyte was spiked into 5 mL deionized water and 1.0 g Na₂SO₄ was dissolved in it. ZIF-4 (20 mg) was then added and vortexed for 5 min to adsorb the analytes. The MOF particles were centrifuged at 7000 rpm for 5 min in order to settle down the particles. The aqueous phase was discarded and ACN (1.5 mL) was added onto the sorbent particles, followed by vortexing for 1 min to desorb the analytes into the organic phase. During the following DLLME step, the eluent containing the extracted analytes was centrifuged for 5 min at 7000 rpm and used as the disperser solvent.

2.5.1 DLLME. The ACN phase obtained from D μ SPE procedure was combined with 30 μ L of 1,2-DBE and rapidly injected into a 10 mL conical bottom glass test tube filled with 5 mL deionized water. The emulsion formation facilitated the transferring and preconcentration of the target analytes into the extraction solvent. In order to isolate the organic phase, the cloudy solution was centrifuged (7000 rpm for 5 min) resulting in the sedimentation of the extractant at the bottom of the tube. A volume of 10 \pm 0.5 μ L of the sedimented phase was collected. One microliter of it was injected into the separation system. Fig. 1 shows the extraction procedure.



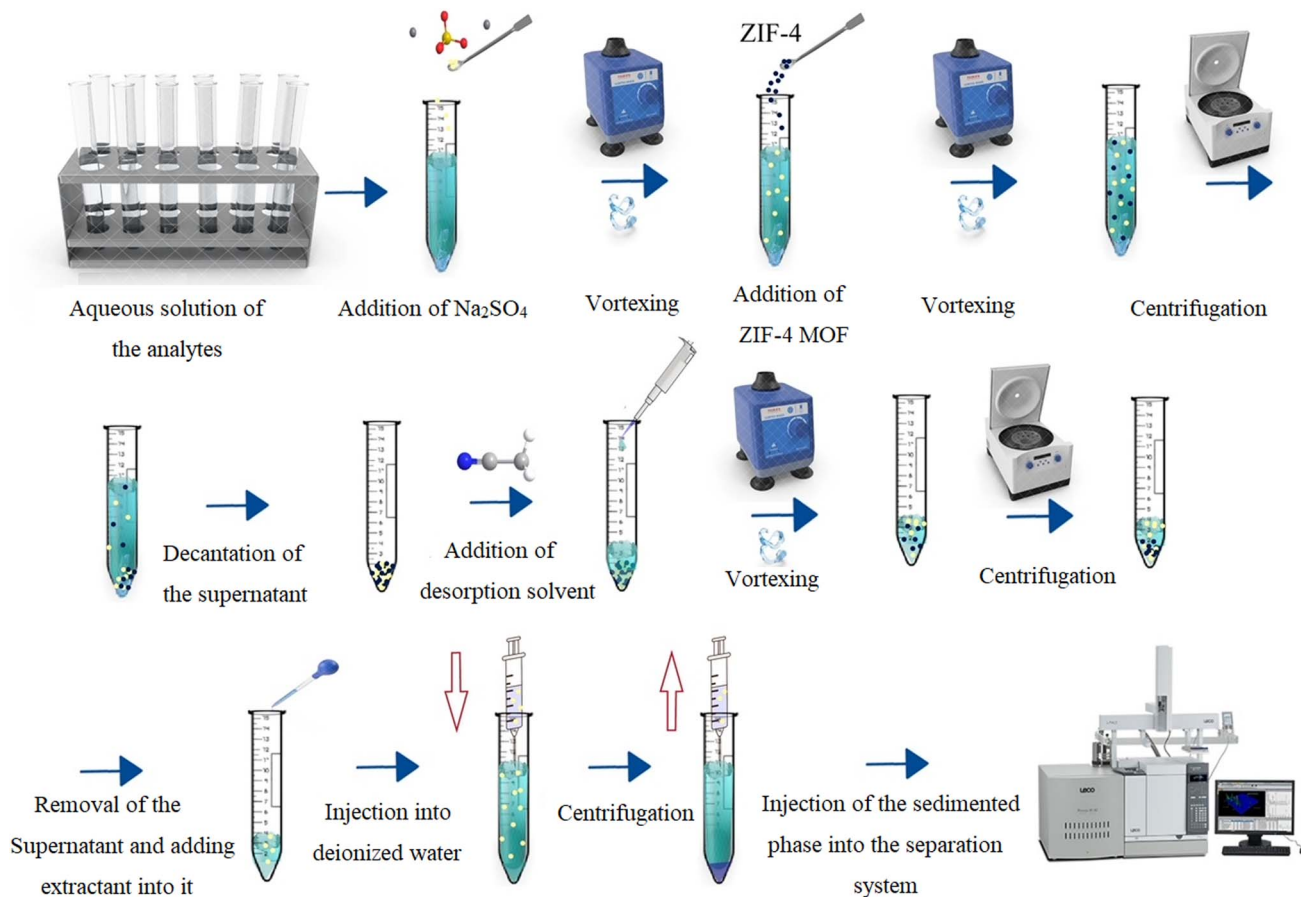


Fig. 1 Extraction procedure steps.

2.6 Calculation of EF and ER

According to eqn (1), the analyte's EF is the ratio of an analyte's concentration in the extracted phase (C_{sed}) to its initial concentration (C_0).

$$EF = \frac{C_{\text{sed}}}{C_0} \quad (1)$$

ER is defined as the percentage of the analyte number transferred from the aqueous phase into the extractant (n_{sed}) to its number in the aqueous sample (n_0) (eqn (2)).

$$ER = \frac{n_{\text{sed}}}{n_0} \times 100 = \frac{C_{\text{sed}} \times V_{\text{sed}}}{C_0 \times V_{\text{aq}}} \times 100 = EF \times \frac{V_{\text{sed}}}{V_{\text{aq}}} \times 100 \quad (2)$$

In this equation, V_{sed} represents the volume of the settled organic phase, while V_{aq} represents the volume of the original aqueous solution.

3 Results and discussion

3.1 Characterization of ZIF-4

XRD analysis is an indispensable technique for characterizing the crystalline nature and confirming the successful synthesis of the target compound. The resulting XRD pattern, shown in

Fig. 2A, displays a series of distinct peaks at approximate 2θ values of 14, 15, 17, 18, 20, 21, 26, 27, 30, 31 and 32° which corresponds to crystallographic planes 121, 202, 221, 023, 311 and 004 of ZIF-4. Based on these peaks, it is concluded that the material is crystalline. Also, the overlapping of the neared pattern and the previous report²⁸ and simulated pattern of ZIF-4 confirms the accuracy of the product.²⁹

The FTIR spectrum of ZIF-4 (Fig. 2B) exhibits characteristic peaks at specific wavenumbers that correspond to different vibrational modes of the MOF functional groups. These peaks provide valuable insights into the molecular structure and bonding interactions present in the material. The peak at 668 cm^{-1} indicates the Zn-N stretching vibration, suggesting strong coordination between zinc and nitrogen atoms in the ZIF-4 framework. The peak at 1677 cm^{-1} points to the C=N stretching vibration, indicative of organic functional group within the imidazole ring. In addition, the peak at 1172 cm^{-1} arises from C-H bond bending, while peaks at 1243 and 1495 cm^{-1} correspond to C-N and C=C bond stretching vibrations, respectively, within the organic framework of ZIF-4.

SEM analysis provides high-resolution images, allowing for detailed understanding the material's surface morphology. This technique is particularly valuable for obtaining microscopic images of ZIF-4. The SEM images in Fig. 2C and D reveal that



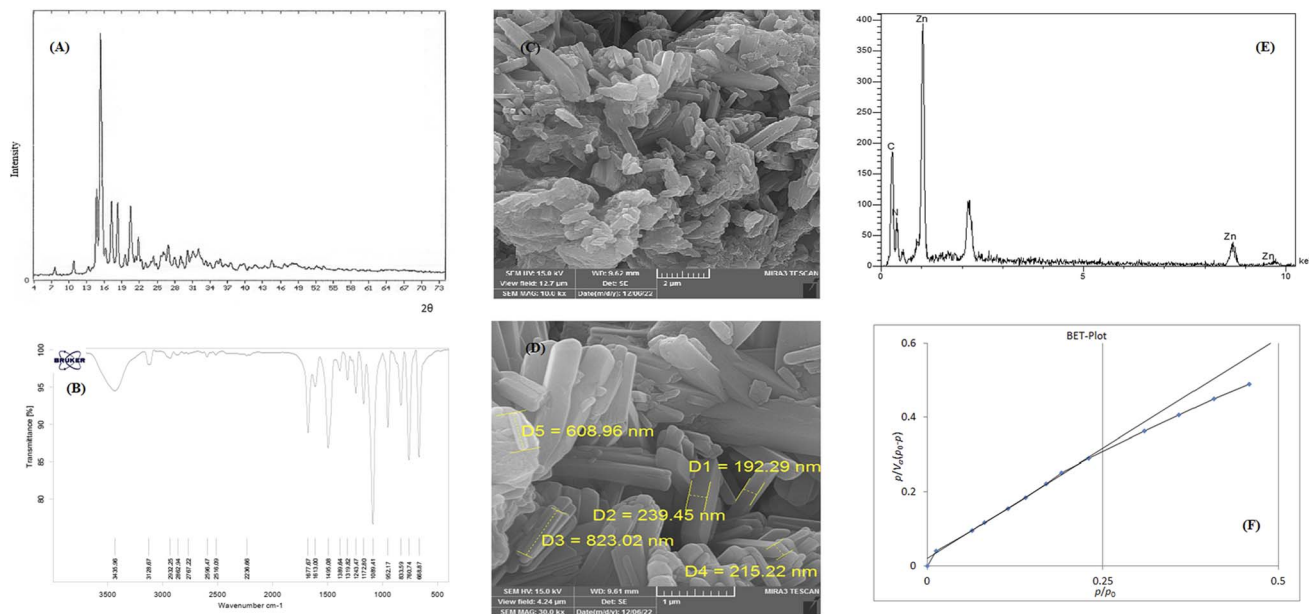


Fig. 2 XRD pattern (A), FTIR spectrum (B), SEM images (C and D), EDX spectrum (E), and BET curve (F) of MOF.

ZIF-4 has a rod-like morphology with a smooth surface, making it a potent adsorbent for the target analytes.

EDX analysis results that are shown in Fig. 2E confirm the presence of carbon, nitrogen, and zinc elements with the relative percentages of 39.25.1% (carbon), nitrogen, 37.57% (nitrogen), and 23.18% (zinc).

The nitrogen adsorption/desorption analysis of ZIF-4 shows that its total pore volume is $0.021 \text{ cm}^3 \text{ g}^{-1}$, its specific surface area is $3.60 \text{ m}^2 \text{ g}^{-1}$, and its average pore diameter is 24.29 nm. These values were determined from the BET plot presented in Fig. 2F.

3.2 Optimization of extraction parameters

Several weights of ZIF-4 (5, 10, 15, 20, and 25 mg) were investigated to develop μSPE procedure to assess the impact of MOF weight. Fig. 3 shows the results of the experiments. The

analyses reveal that 20 mg of ZIF-4 is the optimum sorbent weight. High weights ($>20 \text{ mg}$) result in decreased ER values, possibly due to adsorbent particle agglomeration or inefficient elution of the analytes from ZIF-4 surface. Conversely, lower weights lead to lower ERs as well, likely due to reduced MOF accessibility in solution for adsorption. Consequently, 20 mg of ZIF-4 was chosen for the further optimization steps.

To investigate ionic effect, the ionic strength was adjusted using 1.0 mol L^{-1} solutions of Na_2SO_4 and NaCl , separately. It is shown in Fig. S1 that the introduction of Na_2SO_4 leads to a huge improvement in ERs for all analytes. Then, the effect of Na_2SO_4 concentration was investigated between 5 and 25% (w/v). Following analysis of the results in Fig. S2, concentration of 20% (w/v) was selected due to favorable ERs. Consequently, 20% (w/v) Na_2SO_4 solution was chosen for the subsequent steps.

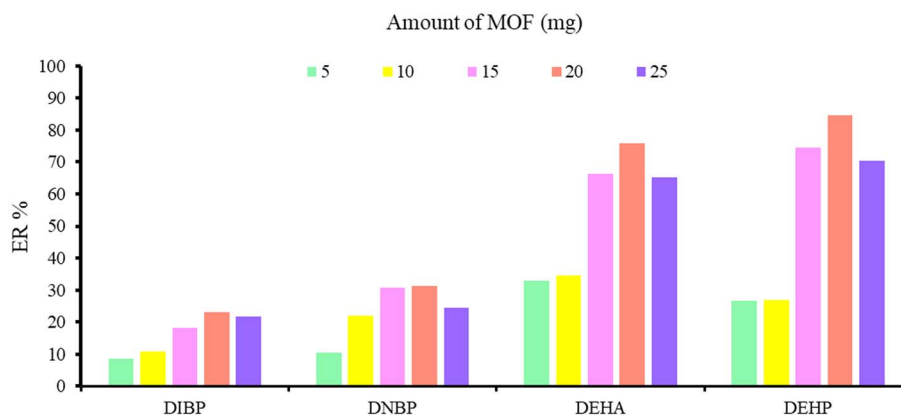


Fig. 3 Optimization of MOF amount. Extraction conditions: μSPE procedure: aqueous solution, 5 mL of Na_2SO_4 solution (1 mol L^{-1}) containing the analytes (without pH adjustment); desorption solvent (volume), ACN (1.0 mL); vortexing time in adsorption and desorption steps, 5 min; and centrifugation time (speed), 5 min (7000 rpm). DLLME procedure: aqueous phase, 5 mL of deionized water (without salt addition or pH adjustment); extraction solvent, 30 μL of 1,2-DBE; and centrifugation time and speed, 5 min and 7000 rpm, respectively.

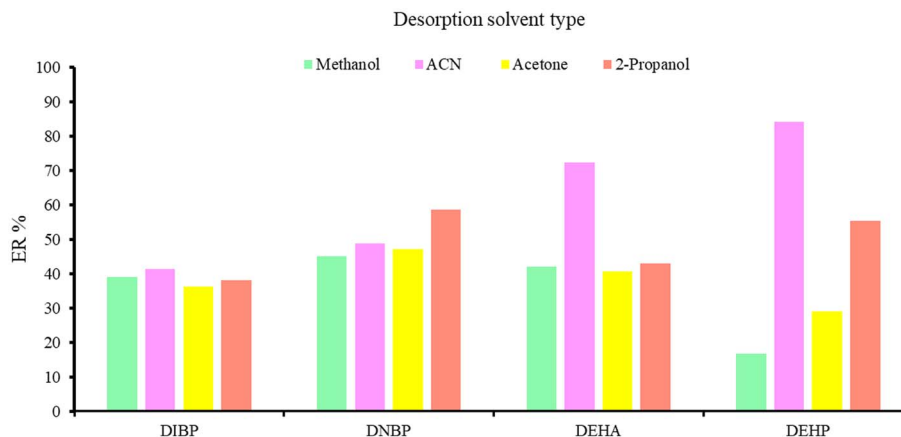


Fig. 4 Selection of desorption solvent type. Extraction conditions: are the same as those used in Fig. S4, except 20% (w/v) Na_2SO_4 was used as the salting-out agent in the D_μSPE step.

To examine the effect of pH on ERs, which can be influenced by changes in the chemical structures of both the MOF and the target analytes, a range of pH values (3 to 11) was investigated using 1 mol L^{-1} solutions of HCl or NaOH. Fig. S3 indicates that the neutral pH of 7 yields the most effective extraction of the target compounds. Consequently, no further pH adjustments were necessary during the optimization experiments.

To ensure optimal adsorption of analytes onto ZIF-4 particles, a vortexing step was employed. To determine the optimal vortexing time, various durations (1, 3, 5, 7, and 9 min) were tested. Fig. S4 demonstrates that a 5 min vortexing time was sufficient to achieve satisfactory desorption. Therefore, the subsequent experiments were conducted using 5 min vortexing time.

To effectively recover the adsorbed analytes from the MOF surface, a suitable desorption solvent is necessary. Four solvents (2-propanol, acetone, methanol, and ACN) were evaluated for their desorption efficiency and dispersing capabilities in the subsequent DLLME step. The experimental data in Fig. 4 indicate that ACN is the most effective solvent due to its superior performance in both desorption and dispersion. To optimize the volume of ACN, a range of volumes (0.5, 1.0, 1.5, and

2.0 mL) were evaluated. As shown in Fig. S5, 1.5 mL of ACN provides the optimum balance between efficient desorption and minimal interference with the DLLME process. Volumes exceeding 1.5 mL could reduce the polarity of the aqueous phase, hindering analyte transferring into the organic phase. Conversely, smaller volumes might be insufficient for complete desorption. Therefore, 1.5 mL of ACN was chosen as the optimum desorption/disperser solvent for subsequent experiments.

To optimize the desorption process and ensure efficient analytes recovery from the MOF surface, a vortexing step was implemented. A range of vortexing times, from 0.5 to 9 min, was investigated to determine the optimal duration. The results (Fig. 5) indicate that 1 min vortexing time is sufficient to achieve effective desorption for most analytes. Therefore, 1 min vortexing time was selected for the subsequent desorption steps.

To further concentrate the analytes after the D_μSPE step, a DLLME step was incorporated. The selection of an extraction solvent necessitates careful consideration of several key properties. These include miscibility with the disperser solvent, low water solubility, and a density exceeding that of water to ensure efficient phase separation through centrifugation. Three

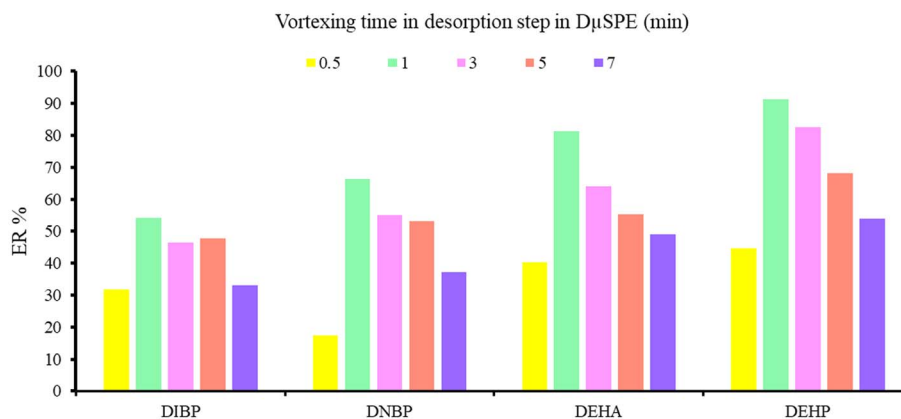


Fig. 5 Optimization of vortexing time in desorption step. Extraction conditions: are the same as those used in Fig. S5, except 1.5 mL ACN was selected as elution solvent.



solvents were considered: 1,2-DBE, chloroform, and 1,1,1-TCE. To obtain a consistent final volume of $10 \pm 0.5 \mu\text{L}$, specific volumes of each solvent were used: $30 \mu\text{L}$ for 1,2-DBE, $34 \mu\text{L}$ for chloroform, and $40 \mu\text{L}$ for 1,1,1-TCE. As shown in Fig. S6, 1,2-DBE provides the best ERs among all analytes.

Different volumes of 1,2-DBE (30, 35, and $40 \mu\text{L}$) were evaluated to determine its optimum amount. $30 \mu\text{L}$ is the most effective volume, as shown by the data in Fig. S7. To investigate the impact of salt content on DLLME efficiency, two salts, Na_2SO_4 and NaCl , were evaluated at a concentration of 5% (w/v). A salt-free solution was also included for comparison. Fig. S8 illustrates that pure water consistently outperforms the salt solutions in extracting all analytes.

Changes in pH during the DLLME process can affect the analytes chemical properties and their ability to be extracted by the chosen solvent. To examine this, the method was performed at various pH levels between 3 and 11. The results (Fig. S9) indicate that deviating from the neutral pH reduces the extraction efficiency of the target compounds. Consequently, the extraction procedure was carried out without pH adjustment.

3.3 Adsorption capacity

The adsorption capacity of ZIF-4 for the studied analytes was calculated using eqn (3).

$$Q_E = \frac{(C_0 - C_E)V}{m} \quad (3)$$

In this equation, C_E (mg L^{-1}) represents the equilibrium concentration of the analyte between the sample and adsorbent, C_0 (mg L^{-1}) is the initial concentration of the analyte in the sample, V is the volume of the solution, and m (g) represents the amount of adsorbent. The adsorption capacities of ZIF-4 for

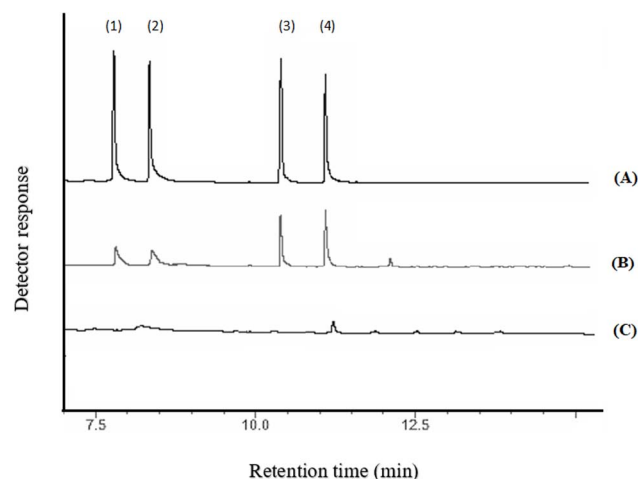


Fig. 6 GC-FID chromatograms of standard solution of the analytes 500 mg L^{-1} of each in methanol (A), aqueous solution ($500 \mu\text{g}$ of each) (B), and wound disinfectant (C). The proposed method was applied on them and $1 \mu\text{L}$ of the final sedimented organic phase was injected into GC-FID, except chromatogram (A) in which organic phase was injected directly. Peaks identification: (1) DIBP, (2) DNBP, (3) DEHA, and (4) DEHP.

Table 1 Quantitative features of the developed analytical method for the analytes

Analyte	LOD ^a	LOQ ^b	LR ^c	r^{2d}	RSD ^e		EF \pm SD ^f	ER \pm SD ^g
					Intra-day	Inter-day		
DIBP	0.23	0.75	0.75–500	0.994	3.70	5.36	305 ± 10	61 ± 2
DNBP	0.28	0.93	0.93–500	0.996	2.39	5.08	345 ± 10	69 ± 2
DEHA	0.20	0.65	0.65–500	0.996	4.30	4.66	370 ± 15	74 ± 3
DEHP	0.16	0.54	0.54–500	0.993	3.82	6.76	475 ± 20	95 ± 4

^a Limit of detection ($S/N = 3$) ($\mu\text{g L}^{-1}$). ^b Limit of quantification ($S/N = 10$) ($\mu\text{g L}^{-1}$). ^c Linear range ($\mu\text{g L}^{-1}$). ^d Coefficient of determination. ^e Relative standard deviation at a concentration of $300 \mu\text{g L}^{-1}$ of each analyte for intra- ($n = 4$) and inter-day ($n = 3$) precisions. ^f Enrichment factor \pm standard deviation ($n = 3$). ^g Extraction recovery \pm standard deviation ($n = 3$).

Table 2 Study of matrix effect in the wound disinfectants spiked at different concentrations

Analyte	Mean relative recovery \pm standard deviation ($n = 3$)		
	Wound disinfectant#1	Wound disinfectant#2	Wound disinfectant#3
All samples were spiked with each analyte at a concentration of $150 \mu\text{g L}^{-1}$			
DIBP	110 ± 4	87 ± 3	112 ± 4
DBP	108 ± 3	109 ± 3	92 ± 2
DEHA	115 ± 5	116 ± 5	98 ± 4
DEHP	104 ± 4	109 ± 4	99 ± 4
All samples were spiked with each analyte at a concentration of $300 \mu\text{g L}^{-1}$			
DIBP	91 ± 3	105 ± 4	93 ± 3
DBP	86 ± 2	110 ± 3	117 ± 3
DEHA	113 ± 5	114 ± 5	110 ± 5
DEHP	114 ± 4	112 ± 4	102 ± 4



DIBP, DNBP, DEHA, and DEHP analytes were obtained to be 0.07625, 0.08625, 0.0925, and 0.11875 mg g⁻¹, respectively.

3.4 Method validation

The proposed method for extracting and preconcentrating phthalate and adipate esters was evaluated under optimal conditions. The method's performance was assessed based on factors such as limits of detection (LOD) and quantification (LOQ), linear range (LR), goodness of fit (r^2), EF, and precision expressed as relative standard deviation (RSD). The calculated LOD and LOQ values ranged from 0.16 to 0.28 $\mu\text{g L}^{-1}$ and 0.54 to 0.93 $\mu\text{g L}^{-1}$, respectively. The method exhibited excellent linearity with r^2 values exceeding 0.99. RSD values varied from 4.66 to 6.76% for inter-day precisions and from 2.39 to 4.30% for intra-day precisions. Furthermore, the ER and EF values ranged from 61–95% and 305–475, respectively. Table 1 summarizes these findings.

3.5 Real samples analysis

This research aimed to develop a method for detecting specific plasticizers in wound disinfectants. Deionized water was used to dilute the samples after they were spiked with known concentrations of plasticizers. The resulting solution was analyzed using GC-FID. Table 2 shows that the method's performance is not significantly affected by the composition of the samples. This indicates that the method is suitable for analyzing plasticizers in these types of samples. Fig. 6 compares the chromatograms of a methanolic standard solution, an aqueous standard solution, and the extracted samples. Interestingly, a peak is observed in the retention time of DEHP in one of the samples used chromatogram. To more identify of the eluted compounds in that retention time, it was also injected into GC-MS. Fig. 7 illustrates GC-total ions current-MS chromatogram of disinfectant solution along with mass data of DEHP and scan 3594 (13.98 min). This data confirm the

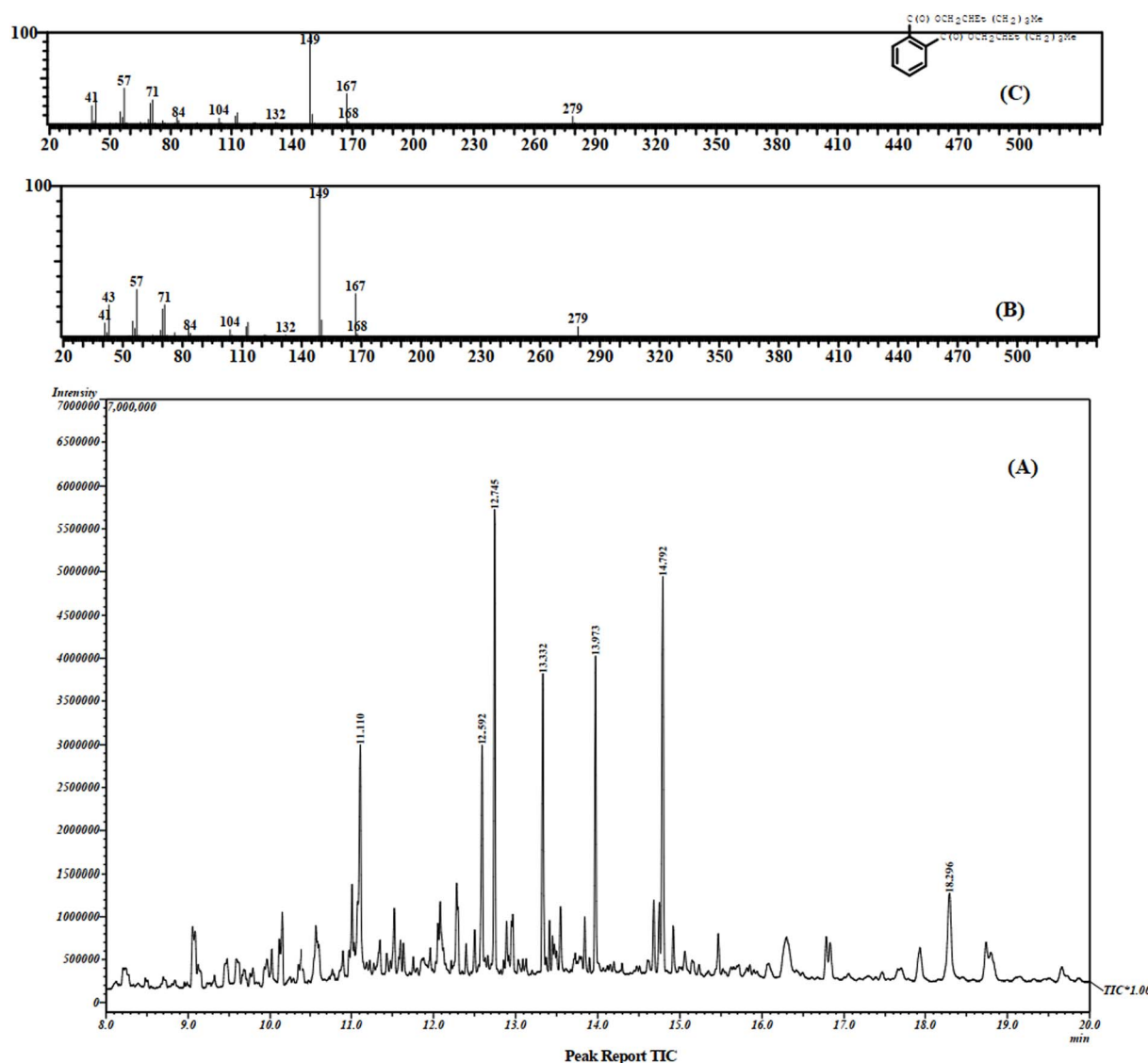


Fig. 7 Typical GC-MS chromatogram of disinfectant after performing the proposed method (A), mass spectrum of DEHP (B), and scan 3594 (retention time 13.98 min) (C).





Table 3 Comparison of the proposed method with the other methods for determination of the plasticizers

Method	Sample	LOD ^a	LOQ ^b	LR ^c	r ^{2d}	RSD ^e	EF ^f	ER ^g	Ref.
VA-EDLME-HPLC-DAD ^h	Fruit juice	5.1–17.8	17.2–59.4	170–4490	0.9994–0.9999	<11	—	—	30
LLF-GC-MS ⁱ	Seawater	0.7–0.32	—	10–1000	0.995<	<10	—	93–97	31
IL-DLLME-HPLC-DAD ^j	White spirit and red wine	1.5–4.2	5–14	10–1000	0.9986–0.9996	0.7–8	51–104	88–104	32
SEAD _μ SPE-DLLME-GC-FID ^k	Sparkling water	0.96–1.40	3.17–4.62	4.38–700	0.995–0.997	3.9–4.6	350–450	70–90	33
IT-SPME-HPLC-UV ^l	Whisky	0.01–0.1	0.03–0.2	0.05–1000	0.9978–0.9995	3.5–8.1	—	92–112	34
SPE-GC-IT-MS ^m	Wine	0.2–14	0.5–25	10–10000	0.9992–0.9997	0.9–10.5	—	96–99	35
HF-LPMF-GC-MS ⁿ	Water	0.4	1.0	1–5000	0.998	9.0	174	—	36
D _μ SPE-DLLME-GC-FID ^o	Wound disinfectants	0.16–0.28	0.54–0.93	0.93–500	0.993–0.996	2.39–4.30	305–475	61–95	Present method

^a Limit of detection ($\mu\text{g L}^{-1}$). ^b Limit of quantification ($\mu\text{g L}^{-1}$). ^c Linear Range ($\mu\text{g L}^{-1}$). ^d Coefficient of determination. ^e Relative standard deviation (%). ^f Enrichment factor. ^g Extraction recovery (%). ^h Vortex-assisted-emulsification dispersive liquid-liquid microextraction-high performance liquid chromatography-diode array detector. ⁱ Liquid-liquid extraction-gas chromatography-mass spectrometry. ^j Ionic liquid dispersive liquid-liquid microextraction-high performance liquid chromatography-diode array detector. ^k Self-effervescence-assisted dispersive micro solid phase extraction-dispersive liquid-liquid microextraction-gas chromatography-flame ionization detection. ^l In-tube-solid phase microextraction-high performance liquid chromatography-ultraviolet detector. ^m Solid phase extraction-gas chromatography-ion trap-mass spectrometry. ⁿ Hollow fiber-liquid phase microextraction-gas chromatography-mass spectrometry. ^o Dispersive micro solid phase extraction-dispersive liquid-liquid microextraction-gas chromatography-flame ionization detection.

presence of DEHP in the studied sample. Concentration of DEHP was $26 \pm 2.1 \mu\text{g L}^{-1}$ ($n = 3$) in the studied sample, based on GC-FID data.

3.6 Comparison with previously published techniques

A comparison of the developed method with existing methodologies is presented in Table 3. This table provides a summary of key performance parameters, including ER, EF, LOD, LOQ, RSD, r^2 , and LR. It was found that the proposed method has comparable or superior LODs and LOQs as well as comparable or lower RSD values with respect to other approaches. The proposed method also demonstrated wider LRs compared to previous approaches. Overall, the proposed analytical approach offers some advantages for the analysis of the selected plasticizers.

4 Conclusions

This study developed a new analytical method to detect and quantify plasticizers that migrate from plastic containers into wound disinfectants. The method combined two extraction techniques, D_μSPE and DLLME, followed by GC-FID analysis. ZIF-4, a specific type of MOF, was employed as an efficient adsorbent in the D_μSPE step. The synthesized ZIF-4 material was thoroughly analyzed using various techniques, including XRD, FTIR, BET, SEM, and EDX. The proposed method exhibited exceptional performance, highlighted by high ERs (61–95%) and EFs (305–475), wide linear ranges, and low detection and quantification limits (0.16–0.28 and 0.54–0.93 $\mu\text{g L}^{-1}$, respectively). The developed technique was successfully applied to analyze the target analytes in the various wound disinfectant samples stored in plastic containers.

Conflicts of interest

There are no conflicts to declare.

Abbreviations

DLLME	Dispersive liquid-liquid microextraction
D _μ SPE	Dispersive micro solid phase extraction
EF	Enrichment factor
FID	Flame ionization detector
GC	Gas chromatography
LOD	Limit of detection
LOQ	Limit of quantification
LR	Linear range
MOF	Metal-organic framework
RSD	Relative standard deviation

Data availability

All the data supporting this article have been included as part of the SI as figures and also the main body of the manuscript. Supplementary information is available. See DOI: <https://doi.org/10.1039/d5ra03198b>.

Acknowledgements

The authors are thankful to University of Tabriz for financial support.

References

- 1 J. Bošnjir, D. Puntarić, A. Galić, I. Škes, T. Dijanić, M. Klarić, M. Grgić, M. Čurković and Z. Šmit, *Food Technol. Biotechnol.*, 2007, **45**, 91–95.
- 2 R. W. Berg and A. D. Otero, *Vib. Spectrosc.*, 2006, **42**, 222–225.
- 3 K. Thummar, R. Vasoya, B. Dama, H. Ladolkar, M. Raval and N. Sheth, *Anal. Chem. Lett.*, 2020, **10**, 93–103.
- 4 N. Ibrahim, R. Osman, A. Abdullah and N. Saim, *J. Chem.*, 2014, **2014**, 682975.
- 5 S. Pezhhanfar, M. A. Farajzadeh, S. A. Hosseini-Yazdi and M. R. A. Mogaddam, *Microchem. J.*, 2023, **195**, 109536.
- 6 L. Ji, Q. Liao, L. Wu, W. Lv, M. Yang and L. Wan, *Anal. Methods*, 2013, **5**, 2827–2834.
- 7 A. Giuliani, M. Zuccarini, A. Cichelli, H. Khan and M. Reale, *Int. J. Environ. Res. Public Health*, 2020, **17**, 5655.
- 8 K. Chou and R. O. Wright, *J. Med. Toxicol.*, 2006, **2**, 126–135.
- 9 P. Gimeno, S. Thomas, C. Bousquet, A.-F. Maggio, C. Civade, C. Brenier and P.-A. Bonnet, *J. Chromatogr. B*, 2014, **949**, 99–108.
- 10 H. Hosney, B. Nadiem, I. Ashour, I. Mustafa and A. El-Shibiny, *J. Appl. Polym. Sci.*, 2018, **135**, 46270.
- 11 M. A. Farajzadeh, S. M. Sorouraddin and M. R. Afshar Mogaddam, Microextraction methods for the determination of phthalate esters in liquid samples: A review, *J. Sep. Sci.*, 2015, **38**, 2470–2487.
- 12 M. Bonini, E. Errani, G. Zerbinati, E. Ferri and S. Girotti, *Microchem. J.*, 2008, **90**, 31–36.
- 13 R. A. Gimeno, R. M. Marcé and F. Borrull, *Chromatographia*, 2003, **58**, 37–41.
- 14 R. Bodmeier and O. Paeratakul, *J. Liq. Chromatogr.*, 1991, **14**, 365–375.
- 15 X. J. Zhu and Y. Y. Qiu, *Adv. Mater. Res.*, 2011, **301**, 752–755.
- 16 K. Kambia, T. Dine, B. Gressier, A.-F. Germe, M. Luyckx, C. Brunet, L. Michaud and F. Gottrand, *J. Chromatogr. B: Biomed. Sci. Appl.*, 2001, **755**, 297–303.
- 17 O. S. Fatoki and A. Noma, *Water, Air, Soil Pollut.*, 2002, **140**, 85–98.
- 18 V. Lo Turco, G. Di Bella, A. G. Potorti, M. R. Fede and G. Dugo, *Eur. Food Res. Technol.*, 2015, **240**, 451–458.
- 19 N. Altunay, A. Elik, M. Tuzen, M. Farooque Lanjwani and M. R. Afshar Mogaddam, Determination and extraction of acrylamide in processed food samples using alkanol-based supramolecular solvent-assisted dispersive liquid-liquid microextraction coupled with spectrophotometer: Optimization using factorial design, *J. Food Compos. Anal.*, 2023, **115**, 105023.
- 20 M. Rezaee, Y. Assadi, M.-R. M. Hosseini, E. Aghae, F. Ahmadi and S. Berijani, *J. Chromatogr. A*, 2006, **1116**, 1–9.
- 21 S. Pezhhanfar, M. A. Farajzadeh, S. A. Hosseini-Yazdi and M. R. A. Mogaddam, *New J. Chem.*, 2021, **45**, 18208–18220.
- 22 M. Tuzen, A. Sari, M. R. Afshar Mogaddam, S. Kaya, K. P. Katin and N. Altunay, Synthesis of carbon modified with polymer of diethylenetriamine and trimesoyl chloride for the dual removal of Hg (II) and methyl mercury ($[\text{CH}_3\text{Hg}]^+$) from wastewater: Theoretical and experimental analyses, *Mater. Chem. Phys.*, 2022, **277**, 125501.
- 23 Y. Kang, L. Zhang, Q. Lai, C. Lin, K. Wu, L. Dang and L. Li, *Polym.-Plast. Technol. Mater.*, 2021, **60**, 60–69.
- 24 S. Pezhhanfar, M. A. Farajzadeh, S. A. Hosseini-Yazdi and M. R. A. Mogaddam, *J. Food Compos. Anal.*, 2021, **104**, 104174.
- 25 A. J. Rascón, P. Rocío-Bautista, D. Moreno-González, J. F. García-Reyes and E. Ballesteros, *Microchem. J.*, 2023, **191**, 108767.
- 26 S. Pezhhanfar, M. A. Farajzadeh, S. A. Hosseini-Yazdi and M. R. A. Mogaddam, *New J. Chem.*, 2023, **13**, 30378–30390.
- 27 J. Zhang, A. Qiao, H. Tao and Y. Yue, *J. Non-Cryst. Solids*, 2019, **525**, 119665.
- 28 B. C. Dhal, S. Hajra, A. Priyadarshini, S. Panda, V. Vivekananthan, J. Swain, S. Swain, N. Das, R. Samantray and H. J. Kim, *Energy Technol.*, 2024, 2400099.
- 29 N. Nasihat Sheno, S. Farhadi, A. Malekib and M. Hamidi, *RSC Adv.*, 2019, **43**, 1956–1963.
- 30 Á. Santana-Mayor, B. Socas-Rodríguez, R. Rodríguez-Ramos and M. Á. Rodríguez-Delgado, *Food Chem.*, 2020, **312**, 125798.
- 31 Q. Zhang, J. Song, X. Li, Q. Peng, H. Yuan, N. Li, L. Duan and J. Ma, *Mar. Pollut. Bull.*, 2019, **140**, 107–115.
- 32 Y. Fan, S. Liu and Q. Xie, *Talanta*, 2014, **119**, 291–298.
- 33 S. Pezhhanfar, M. A. Farajzadeh, A. Mirzaahmadi, S. A. Hosseini-Yazdi and M. R. Afshar Mogaddam, *Chem. Pap.*, 2023, **77**, 4041–4055.
- 34 M. Aghaziarati, Y. Yamini and M. Shamsayei, *Microchim. Acta*, 2020, **187**, 1–10.
- 35 M. V. Russo, I. Notardonato, G. Cinelli and P. Avino, *Anal. Bioanal. Chem.*, 2012, **402**, 1373–1381.
- 36 A. Sarafraz-Yazdi, H. Assadi and W. A. Wan Ibrahim, *Ind. Eng. Chem. Res.*, 2012, **51**, 3101–3107.

